JAAS

PAPER

View Article Online
View Journal | View Issue

Cite this: J. Anal. At. Spectrom., 2022, 37, 1573

Effect of O_2 in plasma gas on parameters of nitrogen MIP-OES†

Oleg V. Komin *[a] and Oleg V. Pelipasov [b]

Received 5th May 2022
Accepted 7th June 2022

DOI: 10.1039/d2ja00154c

rsc.li/jaas

We studied the effect of O_2 content in the range of 0.1–1.2% in plasma gas on the plasma characteristics, the analytical signal and the intensity of the molecular species in nitrogen MIP. The plasma temperature decreases from 4.50×10^3 to 4.39×10^3 K with increasing O_2 content. The Mg(II)/Mg(I) intensity ratio decreases from 1.14 to 0.90, and the electron density decreases from 1.16×10^{14} to 0.85×10^{14}. The intensities of N_2, N_2^+ and NH decrease, and the NO and OH intensities increase when O_2 is added. The influence of O_2 content on the intensity of several atomic and ionic emission lines (covering E_{sum} values from 2.1 to 15.4 eV) of 12 elements has been studied. The intensity of atomic lines with E_{sum} values lower than 6 eV was enhanced in the presence of O_2 but it was suppressed for the ionic lines tested. It was shown that the O_2 addition leads to a decrease in the LOD calculated from atomic lines and to an increase in the LOD calculated from ionic lines.

Introduction

Electrodeless plasma sources (ICP[1] and MIP[2–4]) are widely used for multielement analysis. The characteristics of plasma sources are affected by the type of plasma gas. The argon used for ICP has a high ionization energy, which makes it possible to excite most chemical elements. The nitrogen used in MIP, in contrast, has a low ionization energy, but it can be obtained using nitrogen generators, which reduces the cost of analysis.

In an attempt to improve plasma characteristics in ICP-spectrometry, other gases with chemical and physical properties different from those of Ar have been investigated, particularly mixed gases (Ar–O_2, Ar–N_2, and Ar–He).[5,6] The addition of an impurity to argon affects the plasma characteristics, the analytical signal, and the intensity of the molecular species. Thus, the addition of 10% O_2 increases the ICP temperature by 2000 K,[5] and the addition of 10% N_2 increases the intensity of the Ni(II) 231.60 nm line by an order of magnitude, and the signal/background ratio of Cr(II) 283.50 nm and Co(II) 228.60 nm by two orders of magnitude.[6] There are few similar studies on MIP devoted to the study of the characteristics of 100% air-MIP in the Okamoto cavity,[7] Hammer cavity[8] and MICAP.[9] It is shown that the LOD degrades when nitrogen is replaced by air for all the listed MIP. For the Okamoto cavity, a decrease in the plasma temperature and electron density is also shown.[7]

Moreover, there are several studies devoted to the study of the characteristics of N_2–O_2 MIP. Ohata *et al.* showed that the addition of 20% O_2 to nitrogen MIP in the Okamoto cavity leads to a decrease in the plasma excitation temperature by 700 K.[10] Maeda and Wagatsuma also investigated the parameters of nitrogen MIP in the Okamoto cavity and found a slightly smaller change in excitation temperature (600 K) with the addition of 30% O_2.[11] In both papers, it is said that a drop in temperature leads to a decrease in the intensity of ionic lines and an increase in the intensity of atomic lines due to a shift in the equilibrium between atom and ion densities.

In a recent modelling study of Ar–O_2 MIP generated in a discharge tube crossing a waveguide at the position of the maximum electric field of the TE_{10} fundamental mode, it is noted that the contribution of heating mechanisms depends on the oxygen content.[12] In the mentioned work, up to 1% O_2 in plasma, elastic collision between electrons and argon atoms prevailed, and with increasing oxygen, reassociation of oxygen atoms became the strongest heating mechanism, thus leading to a change in the plasma temperature before and after the addition of 1% O_2.

In this paper, we studied the characteristics of a new spectrum excitation source, which was developed in 2018 based on a cylindrical microwave resonator with the H_{011} wave.[13] The creators of this source note that its structure, discussed in the next section, allows the generation of high-volume plasma, similar to ICP, and is capable of working with high-salt matrices. It should be noted that the effect of O_2 for this source has not been studied previously.

In many laboratories the nitrogen necessary for plasma generation is obtained using a generator based on the PSA

[a]Institute of Automation and Electrometry, Siberian Branch of the Russian Academy of Sciences (IA&E SB RAS), Acad. Koptyug Ave., Novosibirsk, 630090, Russia. E-mail: kominoleg97@mail.ru

[b]Institute of Automation and Electrometry, Siberian Branch of the Russian Academy of Sciences (IA&E SB RAS), 1, Acad. Koptyug Ave., Novosibirsk, 630090, Russia

† Electronic supplementary information (ESI) available. See https://doi.org/10.1039/d2ja00154c

method.[14] The obtained nitrogen is not pure, and contains oxygen as an impurity. The O_2 percentage can be quickly set in the range from 0.001 to 5% by changing the parameters of the nitrogen generator,[15] with 0.5% content being commonly used (99.5% nitrogen purity). There is interest in studying the effect of oxygen, with its content around 0.5%, since this, in addition, will allow us to estimate the effect of the instability of the purity of nitrogen obtained by the generator on the stability of the line intensities. Therefore, in this work, the range of 0.1–1.2% was chosen.

The aim of this work is to study the effect of O_2 content in plasma gas on the plasma characteristics, the analytical signal and the intensity of the molecular species in nitrogen MIP. To this end, dependences of the intensity of analytical lines and molecular bands on the O_2 content were obtained. The MIP characteristics are demonstrated by plasma temperature using Fe as thermometric particles, Mg(II)/Mg(I) intensity ratio and electron density.

Experimental

Instrumental

Microwave plasma excitation used in this work is based on the phenomenon of electromagnetic induction, as in the case of the Hammer cavity and MICAP.[4,8,16] To excite the plasma in this resonator, the magnetic field of the H_{011} wave was used (Fig. 1A). Many different types of modes with different frequencies can be excited in a cylindrical cavity. Based on this, the dimensions of the microwave cavity are selected so that all types of waves except H_{011} are not excited. To increase the strength of the magnetic and electric fields inside the microwave cavity and reduce its size, a dielectric with $\varepsilon > 10$ of magnesium silicate material was installed inside. The nitrogen MIP obtained in this resonator has dimensions and shape similar to those of ICP (Fig. 1B and C). MIP shows low limits of detection (about 0.1–10 μg L^{-1}) and exhibits good stability (<3% RSD).[13] These results are comparable with previously published data for other MIP systems.[4,8,16]

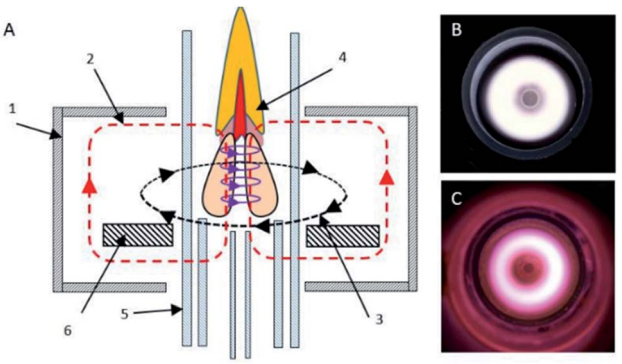

Fig. 1 (A) Scheme of the microwave cavity: 1 – the microwave cavity, 2 – the magnetic field of the wave H_{011}, 3 – the electric field of the wave H_{011}, 4 – the induced electric field, 5 – plasma torch, and 6 – dielectric element. The appearance of the plasma during the axial review: (B) inductively coupled plasma; (C) created nitrogen microwave induced plasma.

To obtain nitrogen, we used a nitrogen generator based on the PSA method. As noted earlier, the oxygen content can be changed by changing the parameters of the generator. In the generator used, it is possible to quickly change some parameters, one of which is the gas flow during desorption. Setting this parameter made it possible to change the oxygen content in the range of 0.1–1.2%. To determine the O_2 content, a gas analyzer, PKG-4 N-K-P (Eksis, Russia), with a flow chamber was used.

A quartz ICP torch (Spectro ML155020, Meinhard, USA) with an injector inner diameter of 1.5 mm was used to create and maintain the plasma in the spectrum excitation source. The applied power was 1.5 kW, the external gas flow rate was 10 L min^{-1}, the intermediate gas flow rate was 0.5 L min^{-1}, and the nebulizer gas flow rate was 0.4 L min^{-1}. A two-pass spray chamber 20-809-0285HE (Glass Expansion, United States) and a concentric nebulizer, One Neb 2 010 126 900 (Agilent, United States), were used to inject the aerosol of the solution. Sample solutions were fed at an uptake rate of 1.5 mL min^{-1} by using a three-channel peristaltic pump (Spetec, Germany).

The radiation from the center of the axial view MIP was imaged by using a quartz lens (83 mm focal length) onto the 2 mm high, 15 μm wide entrance slit of a 1000 mm Paschen-Runge polychromator with non-classical concave diffraction gratings of 2400 lines mm^{-1} and compensated astigmatism (model «Grand», VMK-Optoelectronica, Russia). The radiation from the MIP was recorded simultaneously by assembling the 14 lines of a CCD detector. One line of the CCD detector contains 2048 pixels (pixel – 14 μm × 1 mm). The working spectral range of the spectrometer is 190–350 nm with a resolution of ~10 pm and 350–780 nm with a resolution of ~30 pm.

Reagents and solutions

High-purity water with a resistivity of >18 MΩ cm obtained from a Milli-Q water Direct-Q3 purification system (Millipore Inc., France) was used throughout this work. Multielement solution MES1 (Scat, Russia; Al, Ca, Cd, Fe, Mg, Mn, Na, Cr, Zn, K, and P – 50 mg L^{-1} and Li – 10 mg L^{-1}) after dilution with water up to a concentration of 10 mg L^{-1} (Li – 2 mg L^{-1}) was used as the analyte.

Methods for determining plasma parameters

In the present work, we used the Boltzmann plot method,[17] Saha's equation[17] and Mg(II)/Mg(I) ratio (Mg(II) 280.271 and Mg(I) 285.213 nm lines[18]) to determine the temperature, electron number density, and robustness of MIP at different O_2 contents. The temperature of MIP was calculated from Fe(I) emission lines (248.327, 248.814, 271.903, 299.443, 300.095, 373.486, 373.713, 374.949, 404.581, 430.790, 432.576, and 526.953 nm). The corresponding gA values were taken from the NIST atomic spectra database.[19] Because of the differences in detector sensitivity at each wavelength (Mg(II) 280.271 nm and Mg(I) 285.213 nm), a correction factor must be used with this method.[20,21] Emission signals from W at 280.359 and 285.350 nm ($\Delta\lambda = -0.088$ and -0.137 nm) were recorded for a 2.0% w/w HNO_3 solution, and a value of 0.95 was calculated.

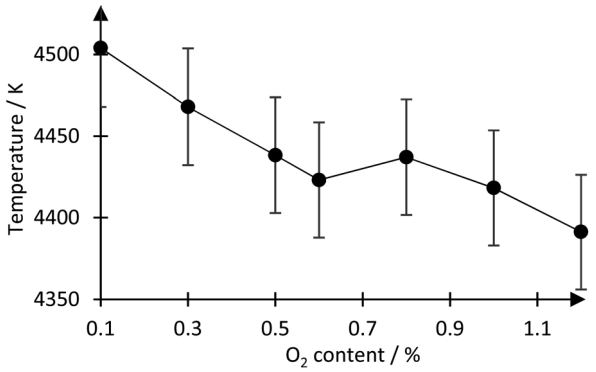

Fig. 2 Effect of O_2 content on the excitation temperature in the MIP calculated from Fe(I) emission lines.

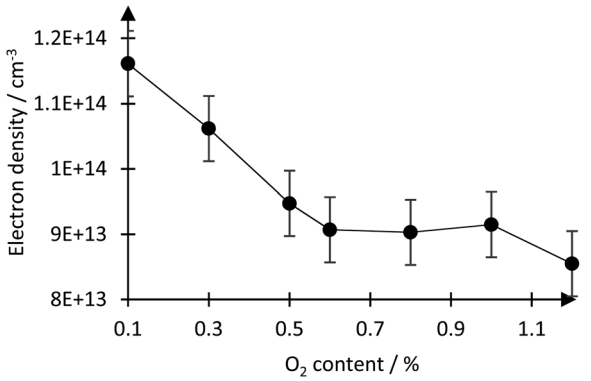

Fig. 4 Effect of O_2 content on the electron density obtained in the MIP.

Results and discussion

Plasma parameters *versus* O_2 content

Fig. 2 shows the excitation temperatures estimated by measuring the signal of Fe(I) as a function of O_2 content. As shown in this figure, the excitation temperature decreased from $(4.50 \pm 0.04) \times 10^3$ to $(4.39 \pm 0.04) \times 10^3$ K with increasing O_2 content. Based on the work on ICP, including modelling of Ar–O_2 ICP,[5,8,22] it can be assumed that the temperature decrease is caused by the lower heat capacity of oxygen (0.92 kJ kg^{-1} K^{-1} for O_2 and 1.04 kJ kg^{-1} K^{-1} for N_2).

Simulation of Ar–O_2 ICP showed that the addition of O_2 up to 100% lowers the plasma temperature. However, experimental data contradict this, showing an increase in temperature in the O_2 content range from 0 to 10%, but the temperature drops as the O_2 content increases from 10 to 100%.[22] The disparity between the simulated and experimental data is partly attributed to the absence of LTE in real plasma.

The MIP also may depart from the LTE when O_2 is added. Therefore, it is necessary to investigate the plasma temperature in a wider range of O_2 content up to 100%. In addition, simulation of the N_2–O_2 MIP would help to understand the reasons for the change in plasma parameters when O_2 is added.

A simple way to monitor the effectiveness of atomization and ionization processes in ICP or MIP is to measure the Mg(II)/Mg(I) ratio (Mg(II) 280.271 and Mg(I) 285.213 nm lines) as detailed by Mermet.[18] The ratio also provides insights into LTE, whereas a Mg(II)/Mg(I) ratio for ICP > 10 suggests a low probability of a plasma equilibrium shift when the sample matrix is injected into the plasma (*i.e.* the probability of plasma-related matrix effects). MIP systems are characterized by lower values of the ratio: Hammer cavity – 0.26–2.01,[2] Okamoto cavity – 0.5–2.5 (ref. 3) and MICAP – 0.5–2.0.[4] The ratio for the obtained MIP is in the range from 1.14 ± 0.06 to 0.90 ± 0.05 (Fig. 3), and therefore, the plasma is in LTE when the O_2 content changes from 0.1% to 1.2%.

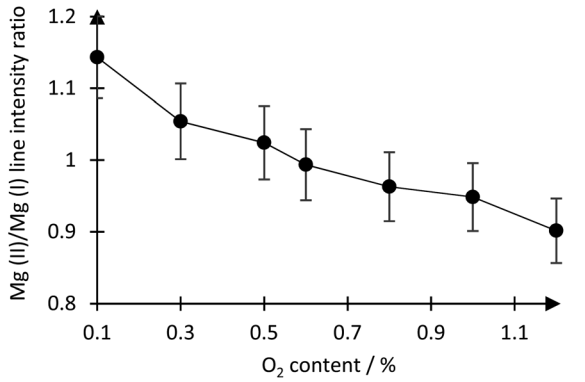

Fig. 3 Effect of O_2 content on the Mg(II)/Mg(I) intensity ratio obtained in the MIP.

Following Saha's equation,[17] a decrease in plasma robustness, together with a decrease in temperature, indicates a shift in the ionization equilibrium towards the formation of atoms. Consequently, the emission intensity of atomic lines should increase, and the emission intensity of ionic lines should decrease.

The obtained temperature values and Mg(II)/Mg(I) intensity ratio were used to calculate the electron density using Saha's equation. With an O_2 content of 0.1% the electron density was $(1.16 \pm 0.05) \times 10^{14}$ cm^{-3} (Fig. 4). These results are comparable with previously published data for other MIP systems.[16,23,24]

Due to the decrease in the electron concentration to $(8.5 \pm 0.5) \times 10^{13}$ with decreasing plasma temperature (Fig. 2), it can be assumed that the main reason for the influence of oxygen is the change in the temperature characteristics of the plasma (heat capacity, thermal conductivity, *etc.*). Otherwise, the dependence would increase when O_2 is added. This is characteristic of matrix influences, where the addition of elements with low ionization energy to the plasma leads to an increase in the electron density. In turn, this leads to a decrease in the kinetic energy of the electrons and, consequently, to a decrease in the plasma temperature.[25]

Intensity of molecular species and analytical signal *versus* O_2 content

The spectrum of the obtained MIP without the introduction of an analyte, the so-called plasma background, consists of structured molecular bands of diatomic molecules: N_2, N_2^+, NH, NO, and OH (Table S1, ESI†).[26] The wavelengths of the analytical

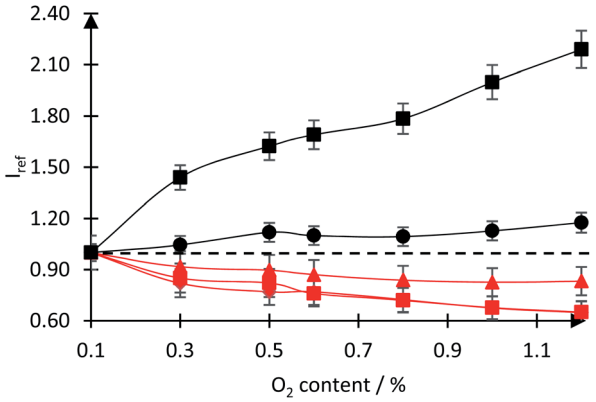

Fig. 5 Effect of O_2 content on the intensity of (▲) N_2, (■) N_2^+, (◆) NH, (■) NO, and (●) OH obtained in the MIP.

lines used in this work are also shown in Table S1, ESI.† The spectra of the obtained MIP at an O_2 content of 0.1 and 1% are shown in Fig. S1, ESI.†

The oxygen necessary for the formation of NO and OH molecules is contained in water, which is the basis of the blank.[13] Since the water content in the plasma is low (sample flow rate: 1.5 mL min^{-1}), the addition of O_2 to the plasma gas (total gas flow rate is approximately 11 L min^{-1}) significantly increases the number of NO and OH molecules in the plasma and, hence, the intensity of their emission (Fig. 5, black curves). The intensity of other molecular bands (N_2, N_2^+ and NH) is affected by a decrease in temperature, which led to a decrease by 17, 35 and 35%, respectively (Fig. 5, red curves).

It is known that a change in plasma temperature and electron density affects the intensity of spectral lines due to an ion–atomic equilibrium shift in plasma.[27] The degree of change in intensity depends on the total excitation energy (E_{sum}) of the spectral line. In this work, to study the effect of O_2 on the intensity of spectral lines, we selected atomic and ionic lines of 12 elements that make up the multielement solution. E_{sum} of these lines has values in the range of 2.1–15.4 eV (Table S2, ESI†).

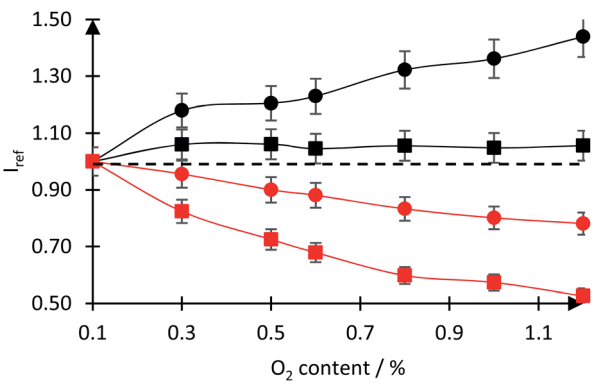

Fig. 6 Effect of O_2 content on the spectral line intensity with E_{sum} of (●) 2–5 eV, (■) 5–6 eV, (●) 11–13 eV, and (■) 14–15 eV obtained in the MIP.

Table 1 Limit of detection (LOD). The LOD was calculated following the 3σ criterion ($n = 10$)

	LOD, μg L^{-1}		
	0.1% O_2	1.2% O_2	$LOD_{1.2\%}/LOD_{0.1\%}$
Al(I) 396.152	1.8	1.4	0.8
Ca(I) 422.672	1.3	0.9	0.7
Cr(I) 428.971	1.2	0.8	0.7
Fe(I) 248.327	26	17	0.7
Mn(I) 403.075	4	3	0.8
Na(I) 589.592	1.4	0.9	0.6
Cd(II) 226.50	60	80	1.3
Cr(II) 283.562	14	17	1.2
Fe(II) 238.203	7	10	1.4
Mn(II) 257.610	3	4	1.3
Zn(II) 206.200	120	260	2.2

The dependence of the intensity of atomic and ionic lines on O_2 content is shown in Fig. 6. Note that the line intensities are the arithmetic means of the intensities within the specified range. As follows from the figure, the intensity of atomic lines (E_{sum} = 2–6 eV) increases up to 1.4 times (Fig. 6, black curves). In turn, the intensity of high-energy (E_{sum} = 11–15 eV) ionic lines is reduced by up to 2 times (Fig. 6, red curves). As mentioned above, this behaviour of the intensities corroborates with the ion–atomic equilibrium shift due to a decrease in temperature.

Changes in the intensity of spectral lines in combination with a change in the intensity of molecular bands affect the LOD of elements. To estimate the degree of change in detection limits, they were calculated following the 3σ criterion, whereas σ is the standard deviation of ten consecutive blank measurements (Table 1). For calculations, the analytical lines of the elements were used in a wide energy range (Table S2, ESI†), including both atomic lines with E = 2–6 eV (growing with the addition of O_2) and ionic lines with E = 11–15 eV (decreasing with the addition of O_2).

Due to the simultaneous increase in the intensity of atomic lines (Fig. 6) and the change in the intensity of molecular bands (Fig. 5), the LOD values calculated from atomic lines are reduced by 20–40% when 1.2% O_2 is added. Conversely, the LOD values calculated from ionic lines increase, for example, for Zn(II) 206.200 nm by a factor of 2.2. Thus, it is possible to reduce the LOD by selecting the O_2 content depending on the analytical lines.

Conclusions

The effects of O_2 content in the range of 0.1–1.2% in plasma gas on the plasma characteristics, the analytical signal and the intensity of the molecular species in nitrogen MIP have been investigated.

The origin of O_2 effects is rather complex due to the simultaneous occurrence of different phenomena. Based on the results of plasma temperature, Mg(II)/Mg(I) intensity ratio and electron density measurements, it was concluded that the

effects of O_2 were primarily attributed to the decrease in plasma temperature. This led to a decrease in the electron density and a shift in the ionization equilibrium towards atom formation.

An increase in O_2 content causes intensity enhancement in most atomic lines presenting lower excitation energies, and intensity suppression in ionic lines of higher excitation energies. At the same time, the intensities of N_2, N_2^+ and NH decrease, and NO and OH intensities increase due to an increase in the number of oxygen atoms and molecules in the plasma. It was found that the O_2 addition leads to a decrease in the LOD calculated from atomic lines and to an increase in the LOD calculated from ionic lines. This should be taken into account when performing multi-element analysis, depending on the analyzed elements and the energies of the available spectral lines.

Future studies will focus on changing plasma parameters by adding oxygen to nitrogen up to 20% (air). Also of great interest is the influence of the O_2 content on matrix effects in nitrogen MIP.

Conflicts of interest

There are no conflicts to declare.

Acknowledgements

The authors are sincerely grateful to VMK-Optoelektronika for the equipment provided. The research was supported by the Ministry of Science and Education of the Russian Federation.

References

1 S. Ghosh, *Asian J. Pharm. Anal. Med. Chem.*, 2013, **3**, 24–33.
2 D. A. Goncalves, T. McSweeney and G. L. Donati, *J. Anal. At. Spectrom.*, 2016, **31**, 1–31.
3 Y. Okamoto, *Anal. Sci.*, 1991, **7**, 283–288.
4 K. M. Thaler, A. J. Schwartz, C. Haisch, R. Niessner and G. M. Hieftje, *Talanta*, 2018, **180**, 25–31.
5 I. Ishii and A. Montaser, *J. Anal. At. Spectrom.*, 1990, **5**, 57–60.
6 A. Montaser, R. L. Van Hoven and R. M. Barnes, *Crit. Rev. Anal. Chem.*, 1987, **18**, 45–103.
7 Z. Zhang and K. Wagatsuma, *J. Anal. At. Spectrom.*, 2002, **17**, 699–703.
8 M. R. Hammer, *Spectrochim. Acta, Part B*, 2008, **63**, 456–464.
9 H. Wiltsche and M. Wolfgang, *J. Anal. At. Spectrom.*, 2020, **35**, 2369–2377.
10 M. Ohata, H. Ota, M. Fushimi and N. Furuta, *Spectrochim. Acta, Part B*, 2000, **55**, 1551–1564.
11 T. Maeda and K. Wagatsuma, *Microchem. J.*, 2004, **76**, 53–60.
12 M. Baeva, *et al.*, *J. Phys. D: Appl. Phys.*, 2021, **54**, 1–15.
13 O. V. Pelipasov, *Anal. Control*, 2019, **23**, 24–34.
14 S. Ivanova and R. Lewis, *Chem. Eng. Prog.*, 2012, **108**, 38–42.
15 A. Schulte-Schulze-Berndt and K. Krabiell, *Gas Sep. Purif.*, 1993, **7**, 253–257.
16 N. Chalyavi, P. S. Doidge, R. J. S. Morrison and G. B. Partridge, *J. Anal. At. Spectrom.*, 2017, **32**, 1988–2002.
17 V. Lochte-Holtgreven, *Methods of Plasma Research. Spectroscopy, Lasers, Probes*, Mir. Moscow, 1971.
18 J. M. Mermet, *Anal. Chim. Acta*, 1991, **250**, 85–94.
19 NIST, *NIST Atomic Spectra Database*, **https://physics.nist.gov/PhysRefData/ASD/lines_form.html**, (accessed 7 December 2021).
20 F. V. Silva, L. C. Trevizan, C. S. Silva, A. R. A. Nogueira and J. A. Nóbrega, *Spectrochim. Acta, Part B*, 2002, **57**, 1905–1913.
21 E. Abad-Penã, M. T. Larrea-Marín, M. Villanueva-Tagle and M. S. Pomares-Alfonso, *Spectrosc. Lett.*, 2016, **49**, 19–22.
22 M. Cai, D. A. Haydar, A. Montaser and J. Mostaghimi, *Spectrochim. Acta, Part B*, 1997, **52**, 369–386.
23 A. J. Schwartz, *J. Anal. At. Spectrom.*, 2016, **31**, 440–449.
24 O. V. Pelipasov and E. V. Polyakova, *J. Anal. At. Spectrom.*, 2020, **35**, 1389–1394.
25 E. V. Polyakova, Y. N. Nomerotskaya and A. I. Saprykin, *J. Anal. Chem.*, 2020, **75**, 474–478.
26 K. Jankowski, E. Reszke, *Microwave Induced Plasma Analytical Spectrometry*, Cambridge R. Soc. Chem., 2010, 12, pp. 264.
27 P. W. J. M. Boumans, *Spectrochim. Acta, Part B*, 1982, **37**, 97–126.